

Table 3. Solutions obtained at points α , β , and γ , bounding the zone of intersection in Fig. 2.

Point	Fraction of r-process synthesis occurring promptly, early in the history of the galaxy	Fraction of r-process synthesis due to continuous addition at a constant rate	Fraction of r-process synthesis contributed by a "last-minute" addition, shortly before collapse of the solar nebula	Time interval between the last event of nucleosynthesis and the onset of xenon retention in meteorites (millions of years)	Galactic age (billions of years)
α	0.87	0	0.13	179	8.0
β	.89	0	.11	176	8.7
γ	.81	0.08	.11	176	8.8

thesis and the galactic age for each of the points α , β , and γ . Within this model, the galactic age lies between 8.0 and 8.8 billion years. The interval of formation of the solar system ΔT is between 176 and 179 million years. Prompt synthesis early in the history of the solar system seems to account for the bulk (81 to 89 percent) of r-process synthesis; very little is due to the continuous mode of synthesis (between 0 and 8 percent); "last-minute" synthesis contributes from 11 to 13 percent of the total r-process material ever produced.

If the whitlockite from the St. Severin meteorite has actually suffered xenon loss, then the value 0.035 reported by Wasserburg *et al.* for the ratio of Pu^{244} to U^{238} at t_0 is an underestimate of the actual value. We can then compute the maximum value for this quantity that is still compatible with the model. Curve VI is the extreme right-hand limit for curves based on Eqs. 2, 4, 5, and 6. It assumes what are considered to be extremum values for the various parameters (Tables 1 and 2). Likewise, curve IX is computed with extremum values chosen to maximize the value of $(\text{Pu}^{244}/\text{U}^{238})_{t_0}$ and still nearly intersect curve VI. No intersection is possible for values of $(\text{Pu}^{244}/\text{U}^{238})_{t_0}$ greater than 0.047, which therefore becomes the upper limit for this ratio consistent with the three-mode model for nucleosynthesis.

An exponentially decreasing mode of nucleosynthesis has been suggested by Fowler and Hoyle (1), but such a model is insufficient in itself to account for the isotopic data. If the "continuous" mode of the model proposed here were exponentially decreasing in intensity, rather than constant, the basic conclusions of this report would be unaltered.

If the "last-minute" synthesis consisted of not one but two local events spaced rather closely in time, then larger values for the primitive ratio of Pu^{244} to U^{238} might be allowed. From the work of Minkowski (16), it is esti-

mated that a typical supernova should enrich an area containing substantially less than 10^{-7} of the galactic mass with r-process debris before becoming sufficiently dilute to blend into the continuum. With the present rate of about one Type-I outburst every 300 years, the possibility of contamination by two nearly coincident supernovae appears to be highly remote.

One of the implied assumptions in these calculations is that the production rates in each of the three modes is the same for both iodine and the transuranic elements. If there were systematic differences in conditions and durations of individual events comprising these three modes, then differences might exist in the fractions A , B , and C for the various elements. If differences do exist, the search for them should center on iodine since this element differs greatly in mass from the other nuclides. Curve X (Fig. 2), computed from Eqs. 3 through 6, is based entirely on uranium, thorium, and plutonium. Even though data on iodine is not included, curve X intersects the zone of solutions in the figure. Furthermore, according to Dicke (4), stellar elemental abundances indicate that at least 60 percent of the r-process synthesis occurred early in the history of the galaxy. If true, this sets a maximum limit of about 0.3 for the "continuous" B fraction, since, with an A fraction of 60 percent, the "last-minute" C fraction is computed to be 11 percent. Therefore curve X gives a value for the galactic age between 8.5 and 9 billion years, and values for the other parameters are compatible with the previous calculations. Thus it seems that there is no apparent difficulty with the assumption that iodine is produced in constant proportion with the heavy elements during r-process synthesis in each of the three modes of element formation.

Note added in proof: Since submitting this report, I have seen a manuscript by G. J. Wasserburg, D. N. Schramm, and J. C. Huneke, to be

published in *Astrophysical Journal Letters*, which treats the problem in a similar manner and arrives at basically the same conclusions.

C. M. HOHENBERG
Department of Physics, University of California, Berkeley 94720

References and Notes

1. W. A. Fowler and F. Hoyle, *Ann. Phys. N.Y.* **10**, 280 (1960).
2. T. P. Kohman, *J. Chem. Educ.* **38**, 73 (1961); D. D. Clayton, *Astrophys. J.* **139**, 637 (1964).
3. A. G. W. Cameron, *Icarus* **1**, 13 (1962).
4. R. H. Dicke, *Astrophys. J.* **155**, 123 (1969).
5. C. M. Hohenberg, F. A. Podosek, J. H. Reynolds, *Science* **156**, 233 (1967).
6. G. J. Wasserburg, J. C. Huneke, D. S. Burnett, *Phys. Rev. Lett.* **22**, 1198 (1969).
7. E. M. Burbidge, G. R. Burbidge, W. A. Fowler, F. Hoyle, *Rev. Mod. Phys.* **29**, 547 (1957).
8. R. Bernas, E. Gradsztajn, H. Reeves, E. Schatzman, *Ann. Phys. N.Y.* **44**, 426 (1967).
9. D. S. Burnett, H. J. Lippolt, G. J. Wasserburg, *J. Geophys. Res.* **71**, 1249 (1966).
10. C. M. Hohenberg, M. N. Munk, J. H. Reynolds, *ibid.* **72**, 3139 (1967).
11. P. Eberhardt and J. Geiss, *Earth Planet. Sci. Lett.* **1**, 99 (1966).
12. J. H. Reynolds, *Annu. Rev. Nucl. Sci.* **17**, 253 (1967).
13. R. Cayrel and G. Cayrel de Strobel, *Annu. Rev. Astron. Astrophys.* **4**, 1 (1966).
14. A. Sandage, *Astrophys. J.* **135**, 333 (1962); A. O. J. Unsöld, *Science* **163**, 1015 (1969).
15. C. M. Hohenberg, *Earth Planet. Sci. Lett.* **3**, 357 (1968).
16. R. Minkowski, *Annu. Rev. Astron. Astrophys.* **2**, 247 (1964).
17. I thank J. H. Reynolds for his encouragement and helpful discussions during this study. Supported in part by the U.S. AEC under code number UCB-34P32-66.

16 June 1969; revised 6 August 1969

Moon: Infrared Studies of Surface Composition

Abstract. Infrared reflectance studies of small lunar regions reveal several absorption bands which match those of ferrous iron in laboratory spectra of olivines and orthopyroxenes. The craters Kepler and Aristarchus exhibit absorption bands suggestive of orthopyroxene, whereas the background mare material shows a band probably due to olivine.

I here describe observations of lunar regions approximately 7 km in diameter with scanning infrared reflectance spectrometry in the region from 0.8 to 2.2 μm . The 61-inch (155-cm)

telescope of the Lunar and Planetary Laboratory Catalina Observatory was used with a scanning infrared spectrometer (1). All observations were made near full moon to take advantage of the maximum surface brightness of the areas studied. The data-reduction method used (2, 3) can be summarized briefly. For each spectral scan the amplitudes of the six atmospheric transmission "windows" at 0.82, 0.90, 1.05, 1.25, 1.55, and 2.10 μm were measured on the tracings. The sum of the amplitudes of the last four wavelengths was divided into each of the six amplitudes to give relative quantities independent of the absolute brightness (albedo) of the lunar region. The points at 0.82 and 0.90 μm were not included in the sum dividend because their amplitudes are sensitive to small changes in the terrestrial water vapor content during the night. For this reason, these two points in the lunar data have lower weight than the remaining four. For each lunar region, three or four individual scans were obtained, each requiring about 1.6 minutes.

The data reduced in such a way provide infrared color curves with the spectral resolution of medium-bandwidth photometry. The lunar color profiles given here may be interpreted as infrared spectra of low resolution which are nevertheless sufficient for recognition of the very broad absorption bands characteristic of absorbing substances in the solid state.

All lunar data were reduced relative to a standard region on the floor of the crater Plato. In Fig. 1, the quantity plotted on the ordinate is

$$L(\text{point}) - L(\text{Plato})$$

where $L(\text{point})$ is the relative spectral luminance of the lunar region at some wavelength λ and $L(\text{Plato})$ is the relative spectral luminance of the floor of Plato at the same wavelength. All quantities on the ordinate have been multiplied by 1000 to give whole number values. Error bars are indicated for points on one curve (floor of Aristarchus). Errors at points 0.8 and 0.9 μm are larger because these wavelengths are affected by variations through the observing period in the concentration of terrestrial water vapor. I calibrated the color of the standard region in Plato relative to the sun, using α Ursa Majoris as an intermediate comparison. The curve of the ratio of the reflectivity of Plato to that of the sun (Fig. 2) shows a shallow depression (absorption) near 1.1

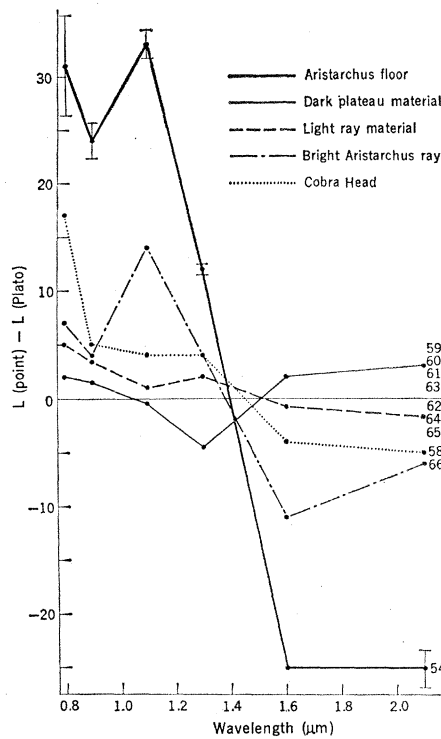


Fig. 1. Colorimetric curves of lunar points in the Aristarchus region. The horizontal line is the reflectivity of the Plato standard point.

μm that may be the same as that found by Tull (4) and Moroz (5). The curves for lunar regions can be reduced relative to the sun by multiplying each wavelength point by the appropriate value of the ratio of the reflectivity of Plato to that of the sun taken from Fig. 2.

Figure 3 shows the locations of several points observed near the crater Aristarchus and on the surrounding structural plateau and mare. Points 59, 60, and 61 lie on the plateau, and point 63 includes similar dark material just north of the crater Prinz. These four points give the color profile (dark plateau material) in Fig. 1, which

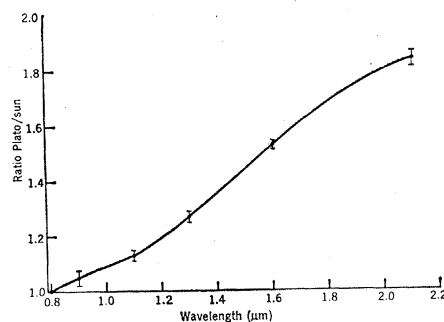


Fig. 2. Reflectivity curve of the floor of the lunar crater Plato relative to that of the sun. The observations were made near a lunar phase angle of zero.

shows a strong depression or absorption at 1.3 μm . Otherwise, the deviation from the horizontal line (the Plato standard point) is small. Points 62, 64, and 65 include mare surface with a moderate amount of ray cover. This has higher albedo than the undisturbed mare surface and is assumed to have a light overcoating of ejecta from Aristarchus and other ray craters. The deviation of these points from the Plato standard point is small, except that they are slightly "bluer" than Plato. Point 66 lies between craters Herodotus and Aristarchus and is heavily covered by ray material from the latter crater. The deviation of the color profile of this area from those discussed above is significant in that there seems to be a magnification of the effect of moderate ray cover on points 62, 64, and 65. The floor of Aristarchus, point 54, also shows an exaggeration of the features in the color profiles noted above with an absorption at 0.9 μm and a large depression at wavelengths greater than about 1.5 μm , both indicative of spectral bands. Point 58, the Cobra Head at the origin of Schroeter's Valley, is different from the others, but it most resembles the curve for moderately ray-covered mare material.

Color curves have also been obtained for the floor of the crater Kepler, a region in the intense Kepler ray system, and a spot in the Oceanus Procellarum which is relatively undisturbed by rays. The similarity in the curves of the craters Kepler and Aristarchus (Fig. 1) is striking. Furthermore, the Kepler ray shows the same absorptions as the Aristarchus ray, whereas the background mare material is nearly neutral relative to Plato. The craters Copernicus and Tycho share the low relative reflectivity at wavelengths greater than 1.5 μm with Aristarchus and Kepler, but they do not show the pronounced absorption at 0.9 μm .

It is possible to make a preliminary interpretation of the colorimetric curves that show well-defined depressions on the basis of the laboratory studies of Adams (6) and Cruikshank (2). Adams found absorption bands, mostly due to electronic transitions in iron in its various valence and crystal coordination states, in the spectral reflectivity curves of olivine and the orthopyroxene families of minerals. Important bands in connection with the lunar data given here are those found in the forsterite-fayalite series at about 1.03 μm (Fe^{2+} in sixfold coordination), in the enstatite-hypersthene series at 0.90 and 1.82

μm (Fe^{2+} in fourfold coordination), and in the complex iron-bearing silicates hornblende and biotite at 0.7 and 2.3 μm (silicon dioxide absorptions). Certain of the bands for iron have also been observed in laboratory samples (2) and are altered by irradiation with a proton flux, thus indicating a change in the valence of the iron (reduction from Fe^{3+} to Fe^{2+}) in the case of a red basalt.

An absorption band that may be attributed to olivine is most likely responsible for the color curve of the dark plateau material observed around Aristarchus (Fig. 1). This is tenable in terms of the presently accepted interpretation that the cover layers on the maria consist of low units (though the upper several meters may be highly

fragmented) of basic (basaltic) rocks. Of the wide variety of minerals studied by Adams (6), only the olivine family and siderite show an appreciable absorption band near 1.3 μm . Siderite, an iron carbonate, is unlikely to occur in the strongly reducing environment at the lunar surface. Thus, the presence of olivine, although perhaps not a unique interpretation, seems the most likely explanation for the observations.

In the color curves of the craters Aristarchus and Kepler, and their rays, two major absorptions coincide closely with those in the spectra of enstatite-hypersthene. The minerals in this family are common in chondritic meteorites and in the rocks that form the upper mantle of the earth. Though it seems that these minerals (or one of them)

may be present at the sites of two major impacts on the lunar surface, it is uncertain whether the minerals represent remnants of the impacting body or material excavated from the lunar mantle and dispersed as rays across the lunar landscape. In either case, the fact that the rays and the interiors of the parent craters show indications of similar composition is of considerable interest.

There is no direct correlation of color profile with albedo or topographic expression of the features studied. The color profiles of some features show absorptions which correlate with physically tenable minerals on the earth. For example, the properties of olivine basalts are consistent with the absorption features found for several mare



Fig. 3. Locations and sizes of lunar points studied in the Aristarchus region. The circles containing the numbers correspond to lunar regions about 7 km in diameter.

regions and also with the chemical analysis of the landing site of Surveyor 5 (7).

We may inquire why the bands in the lunar color profiles reported here have not been seen before. Although a single shallow band has been reported (4, 5, 8), the other bandlike depressions seem to become visible only when very small regions on the moon, each having a certain degree of mineralogical integrity, are observed. The other observers mentioned above have measured the reflectivity of areas somewhat larger than those investigated here.

D. P. CRUIKSHANK
Lunar and Planetary Laboratory,
University of Arizona, Tucson 85721

References and Notes

1. G. P. Kuiper, R. B. Goranson, A. B. Binder, H. L. Johnson, *Commun. Lunar Planet. Lab.* **1**, 119 (1962).
2. D. P. Cruikshank, thesis, University of Arizona (1968).
3. A. B. Binder and D. P. Cruikshank, *Commun. Lunar Planet. Lab.* **5**, 111 (1966).
4. R. G. Tull, *Icarus* **5**, 505 (1966).
5. V. I. Moroz, *Sov. Astron. AJ Engl. Transl.* **9**, 999 (1966).
6. J. B. Adams, *Science* **159**, 1453 (1968).
7. A. L. Turkevich, E. J. Franzgrote, J. H. Patterson, *Jet Propulsion Lab. Tech. Rep.* **32-1246** (1967), p. 119.
8. R. B. Wattson and R. E. Danielson, *Astrophys. J.* **142**, 16 (1965).
9. Dr. A. B. Binder and A. B. Thomson assisted with the observations and reductions, respectively. I thank Drs. S. R. Titley and G. P. Kuiper for valuable criticism. Supported by NASA contract Nsg 61-161 with the Lunar and Planetary Laboratory.

29 January 1969; revised 30 July 1969

(iii) the placement of any stability field is impossible.

The techniques utilized here included optical and x-ray studies of the thermally quenched product, volumetric and electrical measurements *in situ* at high pressure and temperature, high-pressure differential thermal analysis (DTA), and x-ray and optical analysis at high pressure and temperature. In the quench and electrical runs, pressure and temperature were applied by the opposed-anvil system (8) whereas experiments designed to determine volume discontinuities were based on a simple externally heated, piston-cylinder type of apparatus consisting of Bridgman unsupported area-seal steel pistons or tungsten carbide pistons (1.27 cm in diameter) and a closely fitted cylinder of René 41. Gaskets were made of soft annealed nickel disks or rings 0.05 cm thick. Optical studies at high pressure and temperature were made by means of an opposed-diamond anvil system. For DTA experiments argon under pressure was applied to both sample and reference, hermetically sealed in platinum tubes inside a pressure vessel with an inner diameter of 1.27 cm. In all cases temperatures were measured with Chromel-Alumel or Platinel II thermocouples outside the pressure field (except in the DTA experiments). Temperatures and pressures are believed to be accurate to $\pm 2^\circ\text{C}$ and ± 5 to 10 percent, respectively. The techniques used avoid or minimize any tendency for the establishment of pressure gradients in the sample. Flowers of sulfur (sublimed) (Fisher Scientific Company, 99.9 percent purity) and high-purity sulfur (American Smelting and Refining Company, 99.999 percent purity) were used as starting materials. The latter was stored in a vacuum desiccator and was used for 75 percent of all runs and for each of the critical runs.

Figure 1 summarizes our interpretation of the results from over 700 runs made with various types of apparatus. The major features of the liquidus are based on 70 quench runs in the opposed-anvil apparatus in which temperature and load pressure were continuously monitored by an observer. Sets of runs were repeated three times in the region of the liquidus that displays the slight "maximum" about 17 kb. A cusp (intersection of smooth arcs) indicates a triple point formed by the intersection of a solid-solid boundary with the liquidus. Results obtained in

Sulfur Melting and Polymorphism under Pressure: Outlines of Fields for 12 Crystalline Phases

Abstract. *The polymorphism of sulfur has been investigated by static and dynamic methods up to 500°C at 35 kilobars and up to 350°C at 100 kilobars. The melting curve of sulfur to 31 kilobars and phase boundaries of the so-called "4.04-angstrom phase" have been determined. Evidence has been obtained for phase fields of nine new high-pressure forms of sulfur.*

Baak (1) has reported a new "cubic" form of sulfur at pressures greater than 30 kb below the liquidus and another phase with a single diffraction maximum at 4.04 Å. He theorized that the 4.04-Å peak corresponded to the (220) reflection (4.06 Å) of rhombic sulfur and that the crystallization from the liquid state under high pressure was oriented along this plane.

Using a piston-cylinder apparatus with a solid pressure-transfer medium, Geller (2) obtained three crystalline phases (I, II, III) by first melting sulfur under pressure and then inducing crystallization by lowering the temperature. None of these phases matches the cubic phase reported by Baak, although the strongest x-ray peak of phase II occurs at 4.03 Å, thus almost coinciding with the single reflection of Baak's second phase. Sclar *et al.* (3) reported a quenched high-pressure phase which they designated as the "4.04-Å phase," obtained by the use of a belt apparatus and temperature quenching under pressure. The *d*-spacing data of these workers for this phase are practically identical with those of Geller's phase II, and both Sclar *et al.* and Geller point out the similarity of the diffraction patterns to that of the fibrous or ψ form of

sulfur. Geller indexed phase II on an orthorhombic cell and narrowed the space group assignment to three possibilities. Sclar *et al.* reported data on the pressure-temperature range of formation of the liquid and the high-pressure form. Paukov *et al.* (4) observed a sharp decrease in the compressibility of sulfur at 22.5 kb and room temperature; this suggests the possibility of transition to a high-pressure polymorph. These workers also reported a fusion curve out to about 37 kb which showed a maximum at 310°C and 16 kb and a minimum at 290°C and 19 kb.

The results of Geller (2), Sclar *et al.* (3), and Paukov *et al.* (4) and the fusion curves of Susse *et al.* (5) and Ward and Deaton (6) support the qualified suggestion (3) that the 4.04-Å phase exists in equilibrium with the liquid between 30 and 60 kb. A field for this phase probably will have at least two triple points below 30 kb. However, on the basis of Baak's results, Geller's report of quenched phases (I, III), and other fusion curves (7), one may only conclude that thus far (i) one high-pressure crystalline form of S has been found (1-3) (Baak not recognizing it as such); (ii) there have been isolated reports of three other new crystalline phases; and